Chapter 6

A Photometric Fundamental Plane[1]

6.1 Introduction

From the observational view-point, the ingredients of the TF and FP relations are analogous. Magnitudes (for TF), radii and surface brightnesses (for FP) require optical photometric data of similar quality. For galaxies with radial velocity less than ~20,000 km s^{-1}, a ten minute exposure with a high efficiency CCD on a 1m class telescope generally suffices. Also, for observations in clusters, any single exposure provides images for a large number of galaxies (from 2-3 galaxies at the cluster periphery, to 20-30 galaxies at the cluster core). Rotational widths (for TF) or velocity dispersion (for FP) are, on the other hand, much more demanding. Larger telescopes are required than those necessary for the photometry, as well as significantly longer exposures (the median exposure for the spectroscopic observations presented in Table 4.2 was 30 minutes, on the 5m telescope at Palomar Observatory). The number of galaxy spectra that can be obtained with every exposure is also limited (one spectrum at a time for single slit observations, and ~5–10 spectra for multislit spectrographs). While the photometry of a TF or FP program can be economically acquired, the spectroscopy requires an observational investment of roughly one order of magnitude higher cost.

A more "economical" distance-indicator method, that could be build without the use of spectroscopically-derived parameters, but still provide an accuracy comparable to that of the TF and FP relations, would certainly be a very useful tool for observational cosmology. A number of such "economical" methods have been presented in the literature, but none of them is accurate enough to compete with the TF and FP relations, or flexible enough to be applied over a large range of distances. Among the most interesting ones are the methods based on the measurement of the peak of a luminosity function (LF; this can be the the LF of globular clusters or planetary nebulae within a galaxy, or the galaxy LF within a cluster; see Jacoby *et al.* 1992, and references therein), on the Kormendy relation between effective radius and effective surface brightness (Kormendy 1977), and on the measurement of the luminosity of the brightest galaxy in a cluster (Sandage 1972, Sandage & Hardy 1973, Hoessel 1980, Lauer & Postman 1994). Still unexplored is another purely photometric technique, based on a family of relations between

[1]This chapter is an expanded version of the contents of the paper: Scodeggio, M., Giovanelli, R., & Haynes, M.P. 1997, " An Economical Technique for the Estimate of Galaxy Distances: the Photometric Fundamental Plane ", AJ 113, 2087 [copyright 1997 by The American Astronomical Society].

a galaxy effective radius, effective surface brightness, and broadband colors discovered by de Carvalho & Djorgovski (1989).

Here a modified version of the FP relation is proposed, based entirely on photometric parameters. In practice, this methods merges two separate ones, the one based on the Kormendy relation, and the one that uses the LF of the galaxies within a cluster. Taking advantage of the fact that E and S0 galaxies have a peaked LF, it is possible to define for each galaxy Δm as the difference between the galaxy's magnitude and that of the peak of the LF, and use Δm, a distance–independent parameter, in substitution of the velocity dispersion in the FP relation. Although the accuracy of the method is limited, it can nonetheless be a valuable substitute of the FP when the number of velocity dispersion measurements in a cluster is small (less than $\simeq 15$). Because one of its ingredients is the location of the peak of the LF of early type galaxies, this method is based on the assumption that such LF is universal. For the same reason, the method is necessarily limited to the estimation of redshift-independent distances for clusters of galaxies.

6.2 The Kormendy relation

Well known correlations exist between early–type galaxy properties, such as that between luminosity and: r_e (Fish 1964), σ (Faber & Jackson 1976), and μ_e (Binggeli, Sandage & Tarenghi 1984), and the relation between r_e and μ_e (Kormendy 1977). Among those, the Kormendy and the Faber-Jackson relations could potentially be used as distance-indicator relations. However, these correlations exhibit much larger scatter than can be accounted by measurement errors alone. This limits severely their usefulness for distance measurements. Also, this large scatter lead to the idea that early-type galaxies populate a 3–parameter space (the third, missing parameter being the reason for the unexplained scatter in the Kormendy and Faber-Jackson relations), and ultimately to the discovery of the Fundamental Plane relation, independently introduced by Djorgovski & Davis (1987) and by Dressler *et al.* (1987; the $D_n - \sigma$ relation is a projection of the fundamental plane on a two-dimensional space).

The Kormendy relation shows the largest scatter, even greater than the Faber-Jackson relation, and therefore it has been seldom used for distance measurements. However it is an "economical" one, based entirely on photometric parameters, and for this reason it has been recently used by Pahre, Djorgovski & de Carvalho (1996) in two high redshift clusters to obtain an improved version of the classical Tolman test for the expansion of the Universe. Also, for clusters work, the disadvantage of the large scatter is partly offset by the availability of large numbers of objects, that can statistically compensate for the scatter in the derivation of the cluster distances.

Figure 6.1 shows the Kormendy relation for the 409 E and S0 galaxies in the Coma, A1367, and A2634 samples. The 3 samples have been combined assuming that, on average, the 3 clusters are at rest in the CMB reference frame, and then minimizing the chi-square of the linear $\log R_e - \mu_e$ fit, with the individual cluster distances as free parameters. The best linear fit to this data set is given by

$$\log R_e = 0.284(\mu_e - 19.45) + 0.495 - \log h \tag{6.1}$$

where R_e is in kiloparsec, and is computed placing each galaxy at the distance indicated by the cluster redshift, in the CMB reference frame.

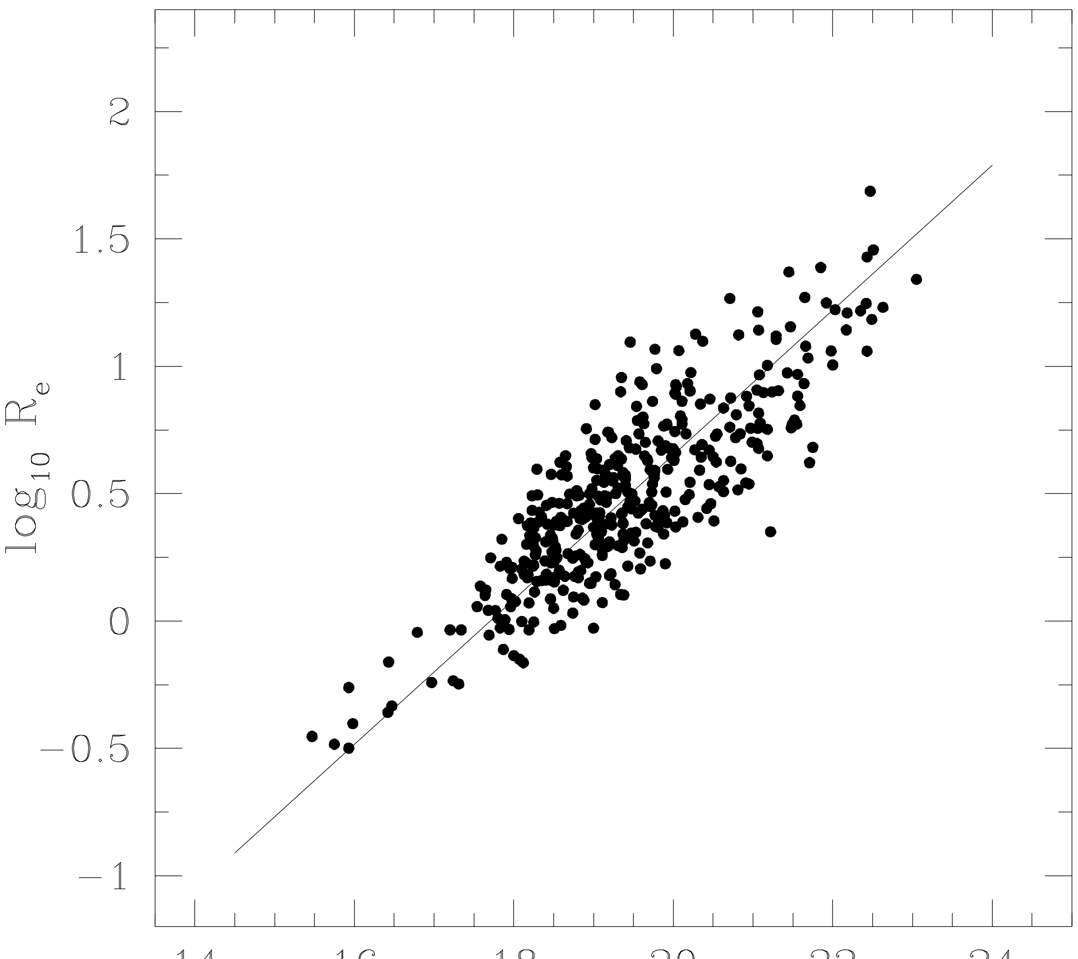

Figure 6.1 The Kormendy relation between the logarithm of the effective radius (in kiloparsec) and the effective surface brightness, for 405 early-type galaxies in the Coma, A1367, and A2634 clusters. The solid line is the best fit to the correlation.

The r.m.s. scatter in $\log R_e$ is 0.19, equivalent to an uncertainty of 0.95 mag. in the distance modulus of a single galaxy. However, the statistical uncertainty in the fit zero point, because of the large sample being used, is only 0.010, equivalent to 0.050 mag, or to an uncertainty of 167 km s^{-1} in the distance to the Coma cluster.

The individual cluster deviations from this mean relation, as derived from the chi-square minimization, and expressed in terms of $\Delta \log R_e$, amount to -0.0036±0.016, 0.028±0.022, and -0.039±0.020, for Coma, A1367, and A2634 respectively. This is equivalent to peculiar velocities of 59 ± 270 km s^{-1}, -450 ± 350 km s^{-1}, and 760 ± 419 km s^{-1} for the 3 clusters.

Figure 6.2 shows the well known fact that the residuals from the Kormendy relation (6.1) are not random: they correlate very well with the galaxy magnitude, or, equivalently, with the galaxy velocity dispersion, bright galaxies exhibiting systematically positive residuals. We remark that the magnitudes used here are derived directly from the observed galaxy light distributions, and are therefore measured independently from the r_e and μ_e parameters. Because of the combination of the large scatter with residuals that are correlated with the galaxy luminosity, the Kormendy relation is severely affected by the cluster population incompleteness bias (Teerikorpi 1987, Sandage 1994a,b). The measured zero point and dispersion of the Kormendy relation depend on the limiting magnitude of the sample, as can be inferred from Figure 6.2 if we imagine the removal of all galaxies fainter than a certain limit. It is therefore very important to derive accurate bias corrections before using the Kormendy relation for cosmological applications like redshift-independent distance measurements.

6.3 The characteristic magnitude

A number of methods are available for the determination of a characteristic magnitude for a cluster sample, using only photometric data. Sandage (1972), and Sandage & Hardy (1973) have used the luminosity of the first ranked galaxy in a cluster to study the linearity of the Hubble flow out to very large distances. These authors claim that all such galaxies have approximately the same luminosity, with a dispersion of only 0.28–0.32 magnitudes (depending on the sample used). A modified version of this distance-estimation method was proposed by Hoessel (1980), and has been used most recently by Lauer & Postman (1994) to study the motion of Abell clusters with $cz \leq 15,000$ km s^{-1}. The uncertainty associated with this method has been estimated to be approximately 16%, or 0.35 magnitudes (Lauer & Postman 1994). Also LF's have been used as distance indicators. Well known is the use of the globular clusters and planetary nebulae LF (see Jacoby *et al.* 1992, and references therein) to derive redshift-independent distances for individual galaxies. The same technique can be applied to the galaxy LF in a cluster, provided that such LF is universal. Since giant E and S0 galaxies and spiral galaxies have been shown to have a Gaussian LF (Sandage *et al.* 1985), its peak M_{peak} can provide an accurate estimate of a characteristic magnitude. Similarly, fitting a Schechter LF (Schechter 1976) to the entire cluster population might provide a characteristic magnitude, in terms of the parameter M_*. Typical statistical uncertainties associated with the determination of M_{peak} and M_* are 0.2 and 0.3 magnitudes, respectively (see, for example, Jacoby *et al.* 1992, and Marzke *et al.* 1994).

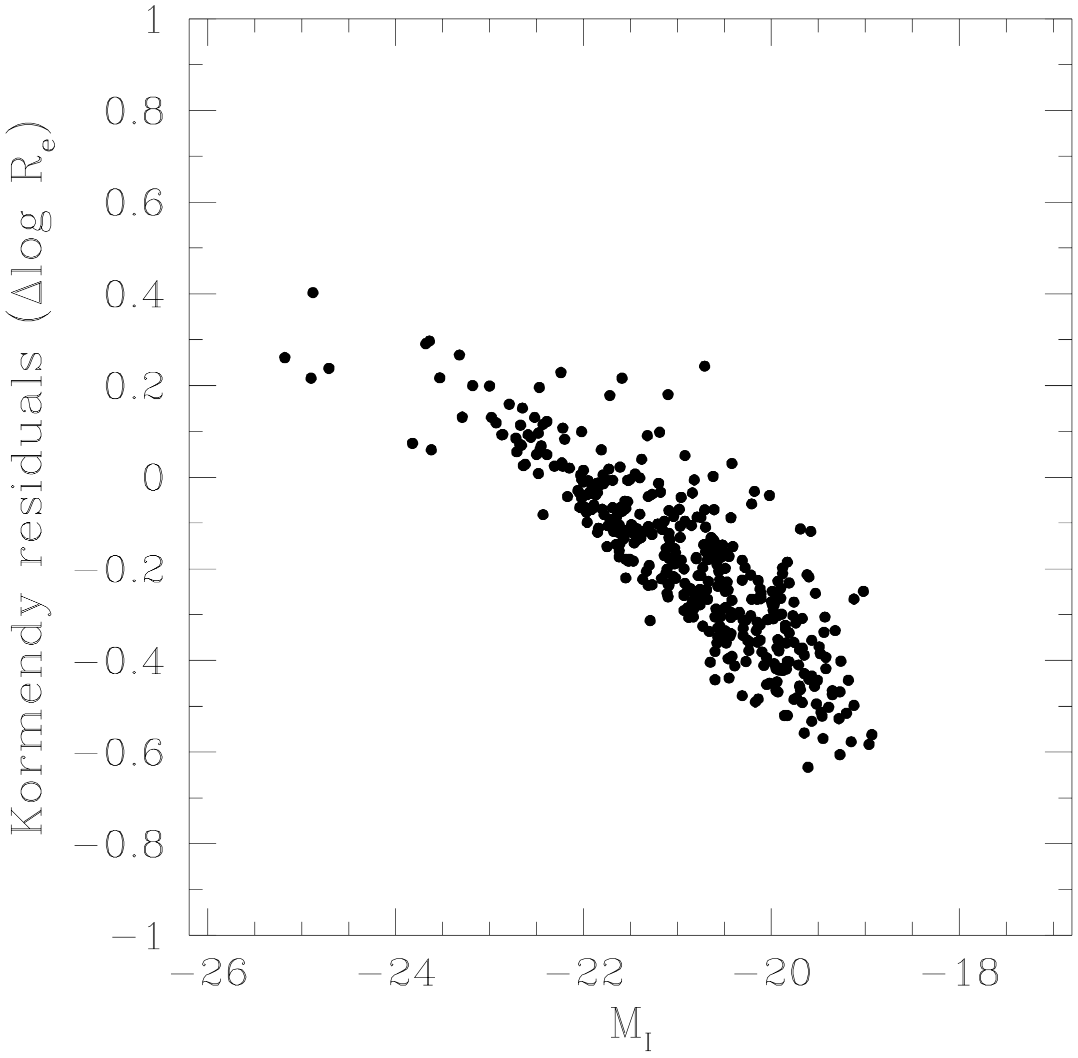

Figure 6.2 The residuals from the best line fit to the Kormendy relation, plotted as a function of the galaxy magnitude.

Table 6.1 Gaussian LF parameters

Cluster	M_{lim}	N	μ	σ_m
Coma	-19.6	187	-20.58	1.275
A1367	-19.6	77	-20.32	1.415
A2634	-19.5	100	-20.56	1.126
All	-19.6	359	-20.55	1.254

6.4 The peak of the luminosity function

Clear evidence that the LF of giant E and S0 galaxies is well approximated by a Gaussian has been presented by Sandage, Binggeli & Tammann (1985) in their study on the Virgo cluster. As these authors showed, it is only when the complete cluster population is considered, including dwarf galaxies, that a Schechter function (Schechter 1976) becomes a better approximation to the LF.

Here the best fitting Gaussian is obtained using a maximum likelihood procedure (see for example Malumuth & Kriss 1986). For a sample complete to a certain limiting magnitude M_{lim}, the likelihood of obtaining the N observed magnitudes M_i within an interval dM of their observed value, when the values are randomly drawn from a Gaussian distribution of mean value μ and dispersion σ_m is given by the product

$$\mathcal{L} = \prod_{i=1}^{N} \frac{N \exp\left[-\frac{(M_i-\mu)^2}{2\sigma_m^2}\right] dM}{\int_{-\infty}^{M_{lim}} N \exp\left[-\frac{(M_i-\mu)^2}{2\sigma_m^2}\right] dM} \tag{6.2}$$

To maximize the likelihood $\mathcal{L}$, we minimize the statistic $S = -2\ln\mathcal{L}$. In practice, since constants in S unrelated to the Gaussian parameters or the data points do not affect the minimization process, we minimize S as defined by

$$S = 2N\left[\ln\left(erf\left[-\frac{M_{lim}-\mu}{\sqrt{2}\sigma_m}\right]\right) + \ln\left(\frac{4\sigma_m}{\sqrt{\pi}}\right)\right] + 2\sum_{i=1}^{N}\frac{(M_i-\mu)^2}{2\sigma_m^2} \tag{6.3}$$

Confidence intervals for the two parameters μ and σ_m are derived from constant chi-square contours (see for example Press *et al.* 1992).

Figure 6.3 shows the results of the Gaussian maximum likelihood fitting to the LF of E and S0 galaxies in Coma, A1367, and A2634. In all graphs the stair-step line represents the observed integral magnitude distribution, while the smooth curve is derived integrating the best fitting Gaussian. The inset show the best fitting Gaussian parameters, and the 68% (1 σ) and 95% (2 σ) joint confidence contours for those parameters. The fit was performed excluding the brightest cluster galaxy, because these galaxies generally appear to have "exceptional" luminosities, being overluminous by at least one magnitude with respect to any reasonable prediction of their luminosity based on an extrapolation of the cluster LF. The fit results are also summarized in Table 6.1,

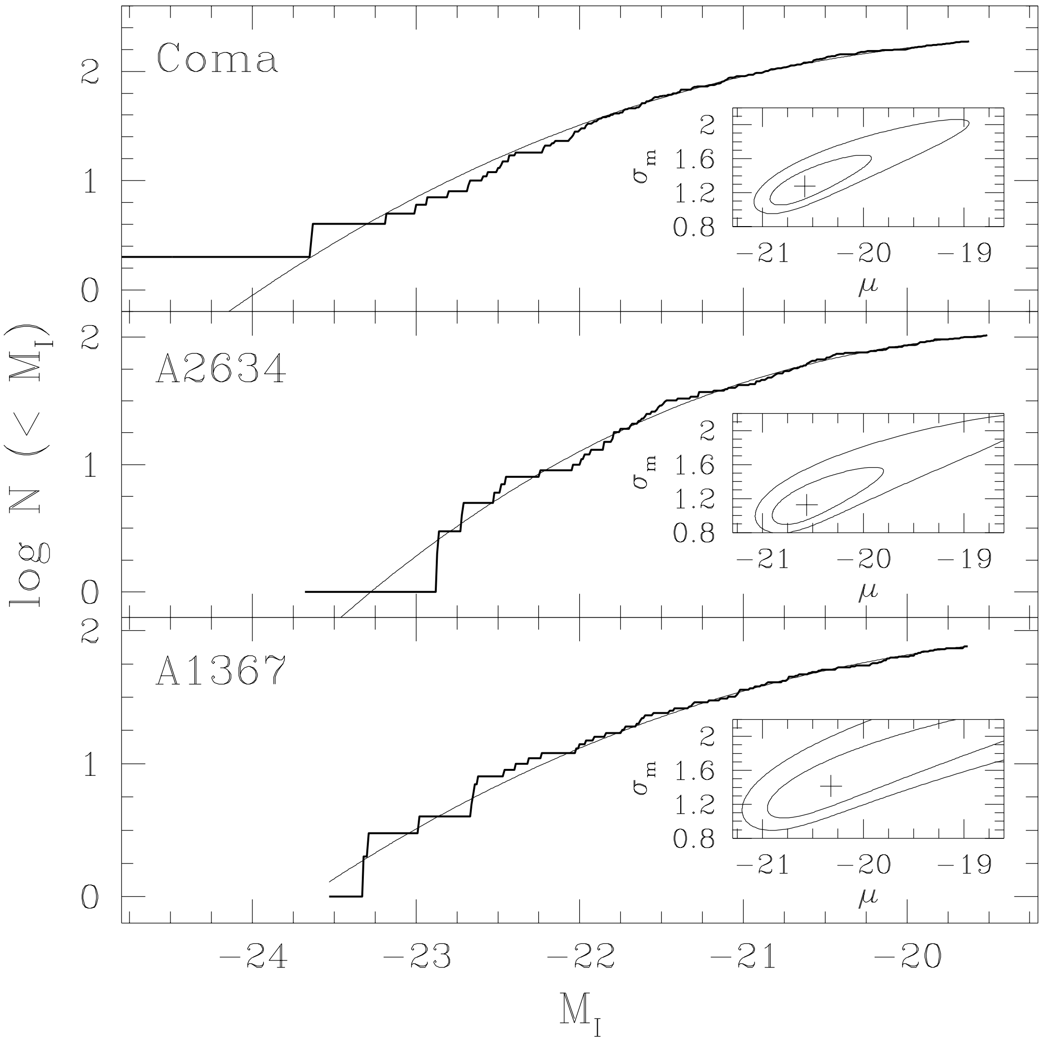

Figure 6.3 Maximum likelihood Gaussian luminosity function fit to the magnitude distribution of the combined sample of early-type galaxies. The fitting was performed excluding the brightest galaxy in each cluster. The stair-steps line gives the observed integral magnitude distribution, while the smooth curve is derived integrating the best fitting Gaussian. The inset show the best fitting Gaussian parameters, and the 68% (1σ) and 95% (2σ) joint confidence contours for those parameters.

that lists the completeness limit of the samples, the number of galaxies brighter than the completeness limit, μ and σ_m from the Gaussian fit.

Because the parameters derived for the 3 separate samples agree well within the statistical uncertainties, it is possible to combine all galaxies in a single sample, and obtain a more accurate determination of the LF parameters. Figure 6.4 shows the results of such a fitting, which are also summarized in Table 6.1: The best fitting Gaussian LF yields $M_{peak} = -20.55$, with a dispersion of 1.25 magnitudes. This is in good agreement with the location of the peak observed in the Coma cluster LF by Biviano *et al.* (1995) and with the Gaussian LF obtained by Sandage *et al.* (1985) for a complete sample of E and S0 galaxies in the Virgo cluster, when an average (B–I) color of $\simeq 2.15$ for early-type galaxies is assumed. The statistical uncertainty in the determination of the Gaussian peak is $\simeq 0.22$ mag. However it still remains to be demonstrated that the location of this peak does not change systematically as a function of cluster parameters like the dynamical evolution state, the richness, or the density of the intra-cluster medium.

6.5 The Photometric Fundamental Plane

It is clear that the two correlations shown in Figure 6.1 and 6.2 can be combined to produce a global relation in the 3-parameter space of $\log R_e$, μ_e, and M. This could be used, in principle, as a distance indication relation, where μ_e would be the distance-independent parameter, and $\log R_e$ and M would be the distance-sensitive parameters, derived from the observed $\log r_e$ and m assuming all galaxies are at the distance indicated by the cluster redshift. Unfortunately, the best fitting plane to the $\log R_e$, μ_e, M relation is given by

$$\log R_e = -0.13\ M + 0.26\ \mu_e + const. \tag{6.4}$$

and the combination of distance-dependent parameters $\log R_e + 0.13\ M$ is quite close to the distance-independent combination $\log R_e + 0.2\ M = \log r_e + 0.2\ m$. Equivalently, the best fitting plane (6.4) is almost parallel to the distance-independent plane

$$m = \mu_e - 5 \log r_e + const. \tag{6.5}$$

that would be populated by a perfectly homologous family of early-type galaxies, making the relation (6.4) of little practical use for distance determinations. However, since a characteristic magnitude can be defined in a distance-independent way for each cluster sample, this relation could be re-written in terms of the magnitude difference ΔM with respect to the characteristic magnitude, instead of the galaxy total magnitude. In this way a relation completely analogous to the FP relation could be obtained, using only photometrically derived parameters, since magnitude differences are distance-independent quantities. Here the mode of the LF of early–type galaxies in clusters is used to define ΔM as the difference between the galaxy's magnitude and that of the peak of the LF. We can then define a fundamental plane in the purely photometric 3-parameter space ($\log\ r_e$, μ_e, ΔM), which we term the Photometric Fundamental Plane or PFP. This plane is closely related to that of the standard FP, translating the dependence of the latter on σ into a dependence on ΔM by mediation of the Faber–Jackson relation.

Figure 6.5 shows an edge-on view of the PFP for the combined sample of Coma, A1367, and A2634 E and S0 galaxies. The best fitting plane, obtained averaging the

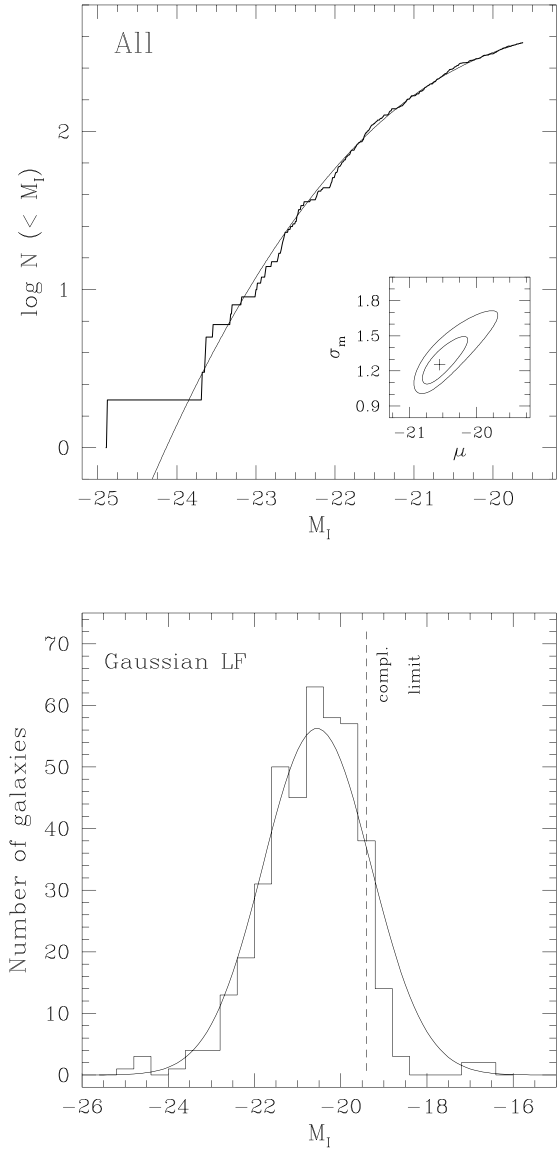

Figure 6.4 Maximum likelihood Gaussian luminosity function fit to the magnitude distribution of the combined sample of early-type galaxies. The fitting was performed excluding the brightest galaxy in each cluster. (a) The stair-steps line gives the observed integral magnitude distribution, while the smooth curve is derived integrating the best fitting Gaussian. The inset show the best fitting Gaussian parameters, and the 68% (1σ) and 95% (2σ) joint confidence contours for those parameters. (b) The histogram shows the differential magnitude distribution, within bins of width 0.4 mag., and the solid line curve shows the best fitting Gaussian. The completeness limit for the sample is shown by the vertical dashed line.

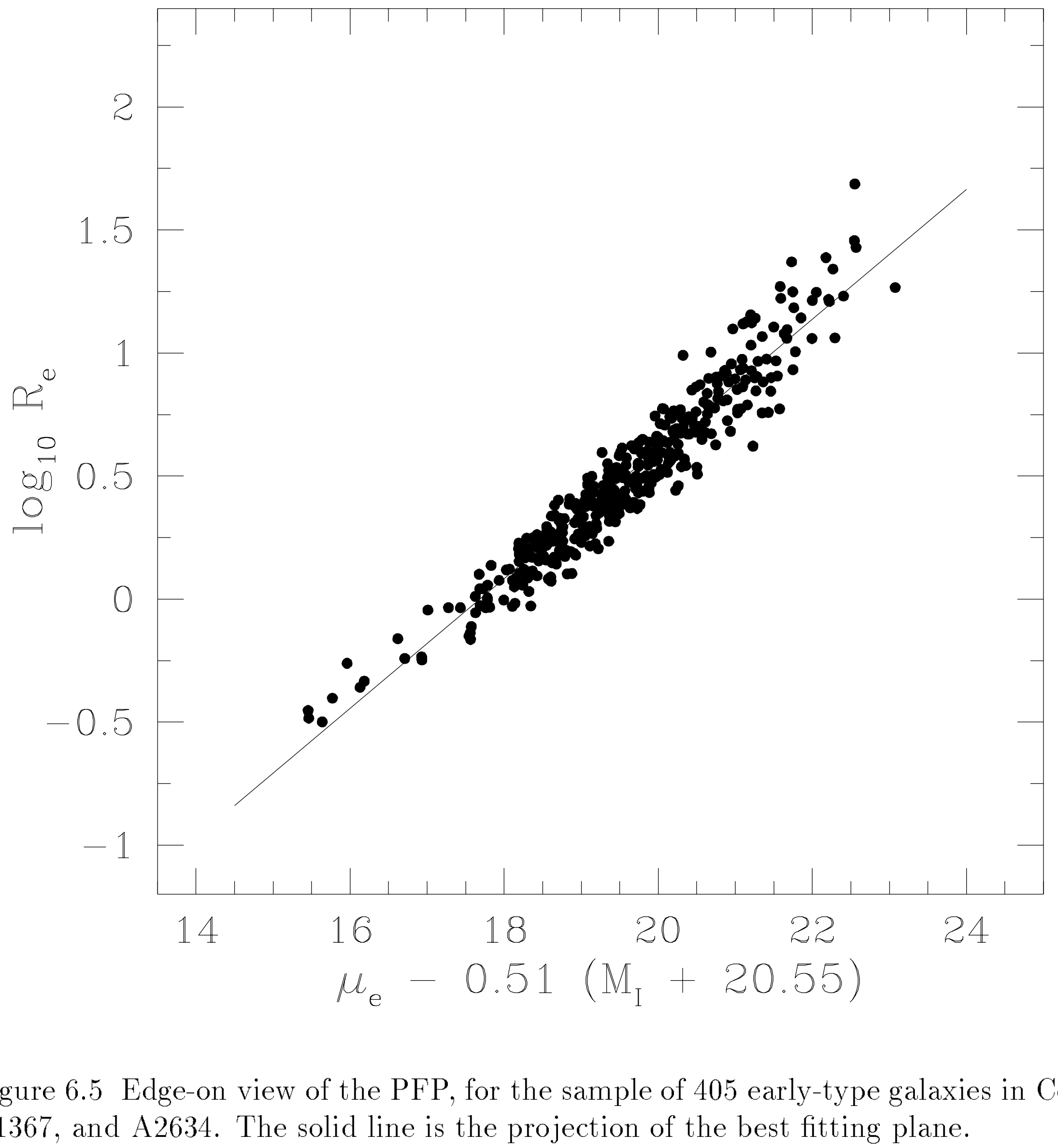

Figure 6.5 Edge-on view of the PFP, for the sample of 405 early-type galaxies in Coma, A1367, and A2634. The solid line is the projection of the best fitting plane.

results of the 3 possible fits that can be performed using one parameter as the dependent variable and the remaining two as the independent ones, is given by the relation

$$\log R_e = -0.13\ \Delta M + 0.264(\mu_e - 19.45) + 0.464 - \log h \tag{6.6}$$

where once again R_e is in kiloparsec, and is computed placing each galaxy at the distance indicated by the cluster redshift, in the CMB reference frame. The statistical problem of finding the best fitting plane to the data is very similar to the one encountered with the FP, because measurement errors in $\log R_e$ and μ_e are strongly correlated, but they have negligible correlation with the measurement errors in ΔM, because total magnitudes are determined independently from the $r^{1/4}$ fit used to determine $\log R_e$ and μ_e (see Figure 6.6).

A hint of non-linearity in the relation is apparent. However, the use of a quadratic relation produces a fit that is not significantly better than the one obtained using equation (6.6). A much larger sample will be required to settle this point. The r.m.s. scatter in $\log R_e$ about the PFP plane is 0.096, which is approximately half the scatter shown by the Kormendy relation, and very similar to the scatter shown by the FP relation, as discussed in section 5.4. This scatter, however, is not the only source of uncertainty in the determination of a cluster distance with the PFP. The uncertainty with which the characteristic magnitude is determined introduces a systematic uncertainty in the determination of the PFP zero-point, that must be added to the statistical uncertainty produced by the scatter. Because this last term scales approximately with the square root of the number of data-points, for a large sample the systematic uncertainty due to the characteristic magnitude determination becomes the dominant source of error in a cluster distance determination. However, the value of the ΔM coefficient in the PFP is such that the effect of this systematic uncertainty on distance determinations performed with the PFP is less severe than it would be on the equivalent determination based solely on the characteristic magnitude. In the latter case the distance uncertainty σ_d is related to the characteristic magnitude uncertainty σ_M by the usual $\sigma_d/d = 0.2 \ln 10\ \sigma_M$, whereas in the PFP case the relation (considering only the characteristic magnitude contribution) is $\sigma_d/d = 0.13 \ln 10\ \sigma_M$, which is $\simeq 1.5$ times smaller.

Figure 6.7 shows a comparison of the accuracy in distance determinations that can be obtained using the Fundamental Plane, the PFP, and the Kormendy relation, as a function of sample size. We assume that in all cases statistical uncertainties scale with the square root of the number of objects used in the fit. The horizontal dashed lines give the accuracy achieved using the FP with a fixed sample size of 10, 20, or 30 galaxies, typical of the samples currently being used for distant and nearby clusters. The scatter in the FP is assumed to be 0.085 (0.43 mag in distance modulus; see Jørgensen *et al.* 1996, Scodeggio *et al.* 1997a, and section 5.4). The two solid line curves give the accuracy achieved using the PFP, for two different values of the uncertainty associated with the determination of the characteristic magnitude (0.25 mag for the upper curve, and 0.15 mag for the lower curve), for a scatter in the PFP of 0.096 (0.48 mag in distance modulus). The dotted line gives the accuracy obtained with the Kormendy relation, for a scatter of 0.19 (0.95 mag in distance modulus), and assuming that the sample completeness bias corrections do not introduce further uncertainties. In this sense, and also because our sample is incomplete at the fainter magnitudes and therefore we are under-estimating the true scatter in the Kormendy relation, this line should be

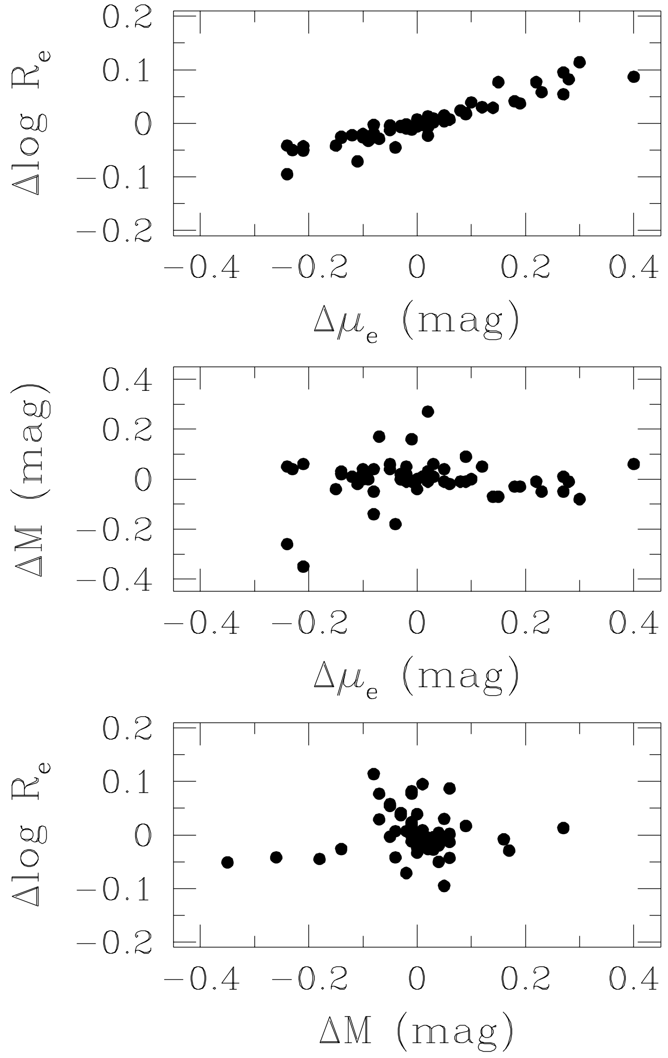

Figure 6.6 The lack of correlation between the total magnitude errors and the other two PFP parameters ($\log R_e$ and μ_e), compared to the correlation between these two parameters errors.

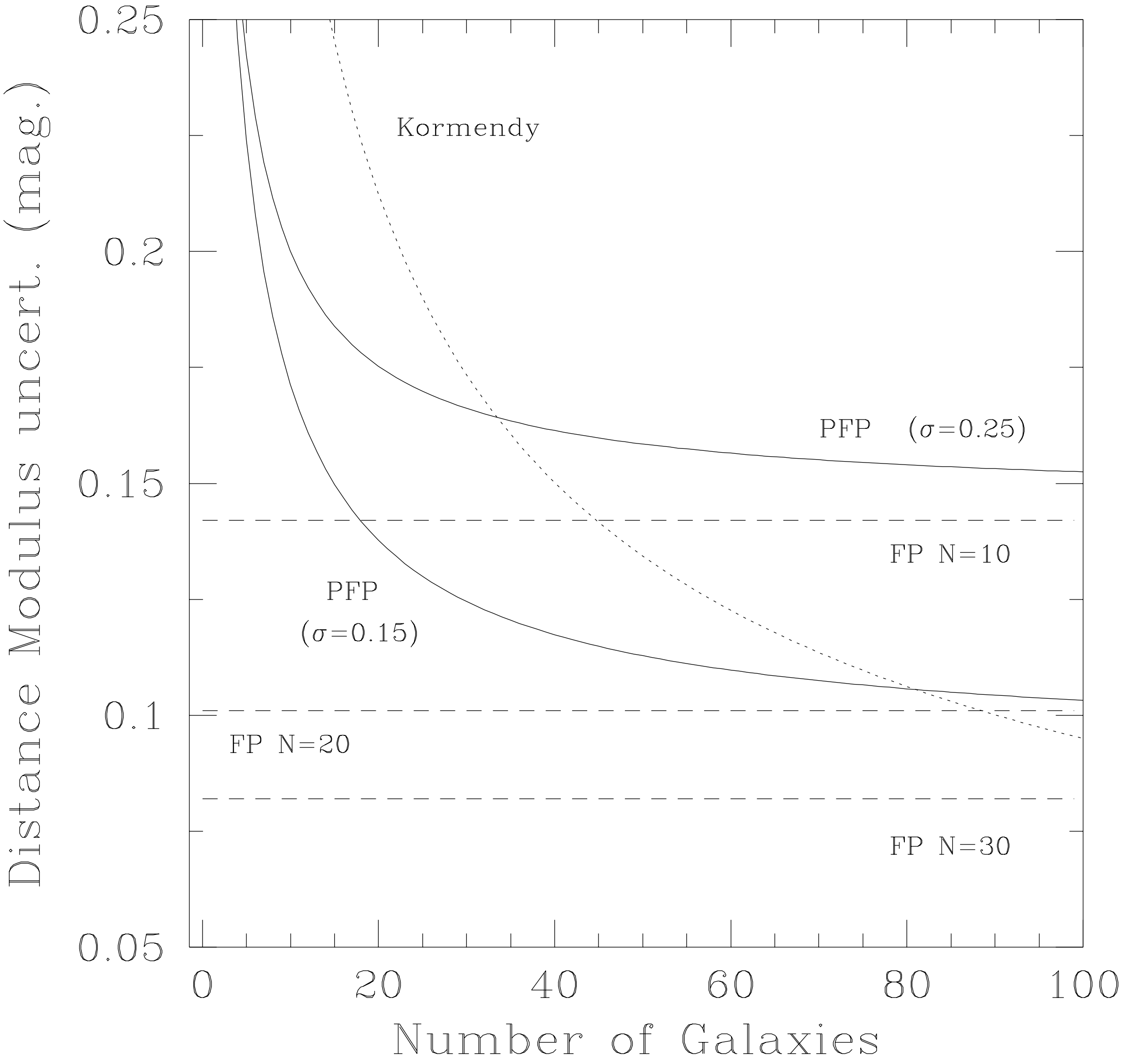

Figure 6.7 Comparison of the accuracy in a distance modulus estimate, as a function of sample size, that can be obtained using the PFP, Kormendy, and FP relation. The horizontal dashed lines give the accuracy achieved using the FP with a fixed sample size of 10, 20, or 30 galaxies (the scatter in the FP is assumed to be 0.085, or 0.43 mag.). The two solid line curves give the accuracy achieved using the PFP, for two different values of the uncertainty associated with the determination of the characteristic magnitude, for a scatter in the PFP of 0.096, or 0.48 mag. The dotted line gives the accuracy obtained with the Kormendy relation, for a scatter of 0.19, or 0.95 mag.

considered an over-optimistic estimate of the accuracy achievable with the Kormendy relation.

6.6 Discussion and Conclusions

As in the case of the relations described by de Carvalho & Djorgovski (1989), the PFP can be understood as a generalization of the fundamental plane relation of early-type galaxies. Although our understanding of the processes of galaxy formation and evolution is still relatively limited, the mass of a galaxy appears to be the fundamental regulating parameter. Because of this, many observable quantities, like the galaxy luminosity, velocity dispersion, metallicity, and broad-band colors, are correlated with the mass, and therefore with each other. The precise form of those correlations is not always well constrained, but a subset exists, including the FP, the PFP and the relation suggested by de Carvalho & Djorgovski (1989), that appears to yield a tighter description of early-type galaxies, within the limits imposed by measurement uncertainties and the intrinsic scatter present among FP-like relations.

The PFP can be a useful tool for observational cosmology. Its most positive characteristics are the relatively modest observational requirements, combined with its potential accuracy. The PFP relation requires only the photometric observations necessary also for the FP relation, without any need for spectroscopic observations. The characteristic magnitude required by the method can be derived from the photometric observations as well, in the form of the mode of the LF, or directly using the magnitude of the n^{th} brightest cluster member. This requirement, however, limits the applicability of the method to clusters of galaxies, and places the ultimate limit to its accuracy.

The accuracy of the PFP zero-point is constrained by the uncertainty in the measurement of the characteristic magnitude. We have seen that, at best, the uncertainty in the PFP zero point can be $\sim$60% of the uncertainty in the characteristic magnitude. Moreover, the PFP is affected not only by the bias intrinsic to the derivation of a template PFP relation, but its zero point is sensitive to biases that might affect the characteristic magnitude. Correlations are known to exist between the luminosity of the brightest galaxy in a cluster and the cluster Bautz-Morgan type (Sandage & Hardy 1973), and also the cluster X-ray luminosity (Hudson & Ebeling 1997). The universality of the LF for clusters is still very much debated. Therefore extreme care will be required for the application of the PFP for distance determination. However the properties of the method used to derive the characteristic magnitude could be in principle derived from the same data used to obtain the PFP relation, and should provide the opportunity to perform stringent consistency checks.

If the characteristic magnitude can be constrained to within 0.3 magnitudes or less, the PFP can offer an accuracy in distance measurements comparable to that of the FP, for a typical FP cluster sample, requiring only one fifth to one tenth of the telescope time. Also important is the fact that the imaging observations do not require a 4-5 meter class telescope (or 8-10 meter telescope, for high redshift clusters), but can be obtained with a 1 meter class telescope.

Finally, one important point must be made regarding the use of the PFP relation at low and high redshift. At low redshift, where the relation would be used to measure deviations from the Hubble flow, the characteristic magnitude must be derived separately for each cluster. At high redshift, instead, where the relation might be used to study evolutionary changes in the mass-to-light ratio of early-type galaxies, peculiar velocities have a negligible effect on the characteristic magnitude. Different cluster samples at the same redshift could thus be combined, improving the determination of the characteristic magnitude, and the accuracy of the PFP method.